Int. J. Simul. Multidisci. Des. Optim. **4**, 63-69 (2010)

DOI: 10.1051/ijsmdo/2010009

Available online at:
http://www.ijsmdo.org

Optimization of Baropodometric Device Instrumentation

Fany Chedevergne[1,a], Alain Burtheret[1], Marc Dahan[1], Bernard Parratte[2]

[1] FEMTO-ST Institute - Department of Applied Mechanics, University of Franche-Comte, 25 000 Besançon, France
[2] Laboratory of Physical Medicine and Rehabilitation, University of Franche-Comte, 25 000 Besançon, France

Received 20 December 2009, Accepted 15 February 2010

Abstract – This article presents the development of a baropodometric device. The aim is to record foot-to-ground force during natural gait. The device consists of an instrumented shoe equipped with force sensors wired to a backpack laptop. The instrumentation should be light, efficient, easy to use for clinical staff and adapted to fit most patients' gait. Thus, we looked to optimize sensor location under the foot and sensor dimensions inside the sole. Numerical simulation and tensile tests lead us to conceive CuBe2 tubular-shaped sensors and specifically-shaped contact aluminum plates. We chose weight/efficiency optimal acquisition system. And we developed a whole treatment process and following graph visualization, optimized over time running and easiness of results reading. Then, we realized dynamic calibration and dead loads weighting to validate our conception. Finally, clinical testing is performed. The gait of the four healthy subjects is presented through the innovating graph visualization.

Key words: Baropodometry; Plantar dynamics; Sensor dimension; Plantar force graph visualization

1 Introduction

Measurement of foot-to-ground force distribution is used for clinical evaluation of foot and gait pathologies. Baropodometric device provides a description of the foot dynamics and thus are clues to detect and predict musculo-skeletic traumas. The various areas of the foot are differently loaded depending on the pathology. For example, if the center of pressure rapidly leaves the heel area to the forefoot, this could indicate a short gastrocnemius muscle and consecutive metatarsal aches (Kowalski [1]).

Mats are ideal to record barefoot walking pressure whereas insoles are generally used for the contact between the foot and the shoe sole. They are both well-known easy-to-use and accurate devices (Allard [2], Cavanagh [3], Herzog [4], Meyring [5], Perry [6], Perttunen [7], Viel [8]). In both case, the number of sensors can reach four per square centimetre, which gives a high spatial precision of the measurement. Sensors are very slim and do not create discomfort. However, these high-technology tools are quite fragile and quite expensive. Moreover, such numerous sensors are not useful. The analysis process of the authors usually runs through a division of the footprint into very few areas, e.g. external and internal parts of the heel, mid-foot, metatarsal heads and toes regions. It wonders the clinical necessity of such numerous sensors.

Various instrumented shoes are also able to record plantar forces (Asphahani [9], Faivre [10], Gross [11], Kirtley [12], Miyazaki [13], Ranu [14], Spolek [15]). The sensor number is limited to one per area of interest. That reduced considerably the data processing duration. Unfortunately most of these authors focused strictly on heel and metatarsal heads. And some discomfort can occur as sensors are located either upon the sole or under the sole. That's why, Asphahani [9] and Faivre [10] proposed instrumented shoes with sole-incorporated sensors. The sensors are inside the sole and spread under the quite entire foot. Used sensors are metallic and based on strain gauge technology which ensures long life-expectancy and cheap price. However, those devices are still under development.

We are here continuing Faivre's work by improving the instrumentation and the data process. Faivre's prototype is covered by the European patent number EP 1 464 281 B1 (Faivre [16]). The mechanical process and the medical interest have been previously validated (Faivre [17]). This article presents the last evolution of these instrumented shoes. Design, treatment process, mechanical calibration and clinical tests are reported. An innovating visualization graph is used to draw the plantar force distribution along the stance phase.

2 Materials

2.1 Design of the baropodometric device

The new prototype (Fig. 1) is based on a pair of Pedar® wild-opening medical slippers. The thickness of the slipper soles has been pierced to incorporate force sensors. Sensors are thicker than the sole thickness so that they contact both foot and ground. The sole move freely around the sensors. During the stance phase, sensors are compressed with no alteration from the sole. The sensor strain is recorded and translated into force. During oscillation phase, the unstrained signal is recorded and used as the zero reference for next compression phase.

The number and locations of the sensors are in accordance with the usual mask used for insoles data analysis (Bertsch

[a] Corresponding author: fany.chedevergne@univ-fcomte.fr

[18], Hennig [19], Meyring [5]). Two sensors are located under the heel, four under the mid-foot, three under the metatarsal heads and two under the hallux and remaining toes. The number of sensors locations has thus been raised from eight to eleven in order to complete the entire sole. Previous prototype focussed on the healthy pathway of the foot stance, ignoring medial mid-foot and little toes. This new set of sensor covers the entire foot and will allow recording any healthy or pathological lay on the floor.

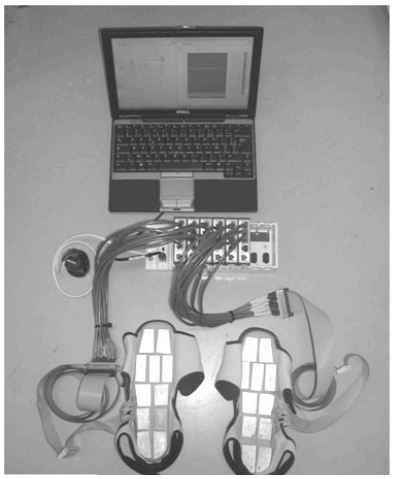

(a) Picture of the baropodometric device: a pair of instrumented slippers, a sensor conditioner and an acquisitioning laptop

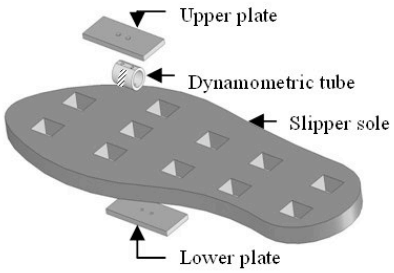

(b) Scheme of the sensors setup and distribution in the slipper

Fig. 1. The new prototype

Sensors are still CuBe2 dynamometric rings turned into dynamometric tubes by increased length from 8 to 16 mm. Nowadays, not only one but two precision strain gauges (resistance of 350 Ω) are pasted on each tube. The tube lies horizontally and from aft forward inside the sole. The main gauge is glued vertically along the medium perimeter. It gets the mechanical compression as well as the unavoidable thermal changes. The second gauge is glued longitudinally so it is negligibly affected by the mechanical compression but gets the same thermal changes. A Wheatstone half-bridge set up allows cutting the caloric effect and keeping out the single compression effect. A National Instrument® conditioner and a LabView® program acquire this output.

The previous metallic box welcoming the dynamometric was source of inconstant mechanical strain result for a same compression force. It is taken away and its role of vertical guideline for the compression is compensated by fixing the dynamometric tube in horizontal position. A bottom plane and an opposite upper plane cut from the tube surface determine the horizontal position. The tube external diameter (12.7 mm) remains at 12.3 mm between the plates in order to overpass the Pedar® slipper sole thickness (11 mm).

Both planes welcome an identical aluminum plate. The upper plate contacts the foot over the sole whereas the lower plate contacts the ground under the sole. During the stance phase, the foot pushes down the upper plate and compresses the tube vertically against the bottom plate lying on the ground. The slipper sole move freely between the two plates without altering the compression process. Each sensor provides the vertical compression force exerted by the foot on its own upper plate, i.e. the vertical reaction force exerted by the ground on its own bottom plate. The eleven upper plates, as well as the eleven bottom plates, cover 95% of the sole surface.

The tube internal diameter (9.7 mm) has been first determined by dimensional optimization through tensile simulation on COMSOL® software (Fig. 2) and then confirmed by reel crash tests on a tensile device (Fig. 3). The plastic threshold was set at 6000 N to ensure the elastic behavior of the tube during ambulation even if the foot hits the ground.

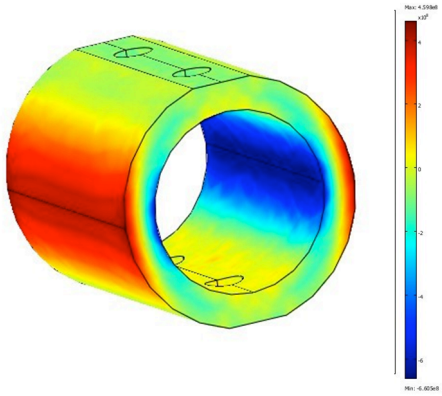

Fig. 2.Tensile simulation

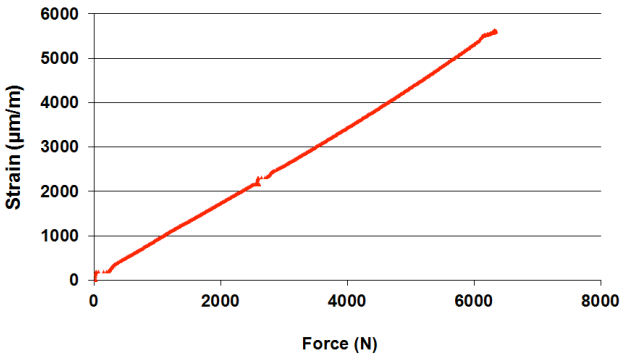

Fig. 3. Force/strain curve of the tensile test

The conditioning system and the acquisition laptop settled in a backpack. This 4 kg amount of mass does not affect the patient's natural kinematics as long as it is less than 10% of the individual's body mass (Grimmer [20]). Patient over 40 kg are free from added gait perturbation.

The treatment process indicates the force recorded by each sensor, the vertical ground reaction force deduced for the entire foot, the plantar pressure distribution under the foot

and the center of pressure location, throughout the entire stance phase.

2.2 Treatment process

To translate the recorded strain into the plantar forces, we developed a complete Matlab® program. This program runs automatically and passes through offset and electronic drift correction, voltage to force translation, force to mass conversion, expression in percentage of body mass, stance phase detection, duration normalization, mean of values and graph plotting.

The offset and drift corrections are based on oscillation phase signals. When sensors are unloaded, each sensor residual signal is recorded and taken as reference. That induces needed initial and final lifted feet phase at the beginning and the end of the walking protocol. The correction started by the initial offset and then assesses a linear drift coefficient applied to the entire trial.

The translation into the exerted force (N) is deduced from previous sensor calibration. The force is then converted into mass (kg) and expressed in percentage of the experimental mass (i.e. body & backpack mass).

The stance phases of each foot are determined between the first moment a sensor yielded a value above 5% of the experimental mass and the last moment before all the sensors yielded a value under 5%. Each stance phase is then normalized over time and sensor signal are kept at every 10% of the stance duration (0%, 10%, 20%, …, 90% and 100%).

Then the mean value of each sensor at each of the 11 instants is processed over all the stance phases of the trial. That gives the evolution of each sensor signal during the mean stance at every 10% of the phase duration. These results are then used to obtain both the classical vertical ground reaction force and the innovating plantar force visualization graph.

2.3 Plantar forces visualization graph

An elaborate plotting function ends the Matlab® program. It draws a one-shot graph presenting the plantar forces distribution evolution throughout the stance phase for each foot.

The eleven instantaneous footprints of the mean stance phase are drawn for each foot. Each footprint is figured by the eleven sensors of the sole. The top row of footprints illustrated the left foot whereas the bottom one stands for the right foot. The stance phases runs from the left side (“0%” footprint) to the right (“100%” footprint), through footprints at every 10% of the phase duration.

The force magnitude exerted on each sensor is indicated in grey. The grey follows a shade scale going darker for every 10% of the experimental mass. White represents less than 10% of the experimental mass and black represents over 100%. This force magnitude scale is indicated at the very top of the graph. The force magnitude is expressed both in a percentage of the experimental mass and in an absolute value of the corresponding actual mass.

The center of pressure is illustrated by a little square on each footprint. This barycenter is assessed and plotted for each footprint provided the instantaneous mass undergone by each sensor.

3 Methods

3.1 Dynamic calibration

The sensors calibration aims to define the force/signal relationship of each sensor. Though apparently similar, each home-made dynamometric tube has its own inherent mechanical behavior.

The calibration used a 6025 Instron® electromechanical universal testing system. The device pushes down the upper plate while the bottom plate lies on a not deformable surface. The contact of the tensile machine was limited to one single sensor at once. Other sensors were not involved in the compression. A trial of five cycles of compression from 50 to 3000 N and back to 50 N has been chosen. Compression speed was set at 50 N/s and sample frequency at 10 Hz.

We first attested that calibration result was repeatable for a same sensor over 5 trials separated by unsetting and setting up of the sensor into the sole. Five random sensors were used and all presented excellent calibration repeatability.

Then, each of the 22 sensors has been calibrated. We observed the strain output of the compressed sensor along the entire test. We also observed the one of the other sensors, uncompressed, to ensure the absence of contact between the sensors.

3.2 Dead loads weighting

Dead loads weighting test consist in laying an inert known mass upon the sole over the eleven sensors at once.

Thanks to available masses, totals of 6 kg, 24 kg and 34 kg were loaded and unloaded until 0 kg, three times. The mean mass and force per sensor was so 0.6, 1.2 and 3.3 kg and 5, 11.6 and 32.4 N. The sample frequency was set at 100 Hz. The strain of each sensor was recorded for 2s. The offset and shift correction were proceeded for each cycle using the signal value of the unloaded phases (0 kg).

Recorded strains were converted into masses using the previous dynamic calibration results for each sensor. The sum of the mass measured by the eleven sensors of the slipper was assessed and compared to the loading masses. The comparison of the results across the cycle indicates the repeatability of the process.

3.3 Clinical testing

Two women and two men (Table 1) between 25 and 29 years old performed a standard return gait task of 10 meters. They had no residual locomotive deficiency from their past medical history. The subject mass was assessed using an eye-level mechanical physician scale.

Table 1. Characteristics of the four subjects

	Sex	Age	Height (cm)	Mass (kg)	BMI*
Subject A	F	29	169	76.5	26.8
Subject B	F	25	162	51	19.4
Subject C	M	27	183	83	24.8
Subject D	M	28	178	67	21.1

* Body Mass Index

	Past Medical History
Subject A	- right ankle: 1 fracture, 2 sprains - left ankle: 1 sprain
Subject B	- right ankle: 1 sprain - left ankle: 1 sprain - left knee: 1 sprain
Subject C	- beginning of scoliosis at adolescence
Subject D	- flat feet at adolescence

Subjects were equipped with the baropodometric device: the two instrumented slippers and the 4-kg backpack. The entire protocol was explained to each of the four subjects and one rehearsal was performed prior to recording three trials.

Subjects began in a seated position with both feet lifted for 3 seconds, stood up on both feet for 3 seconds, walked 10 meters forwards, returned back, stood on both feet for 3 seconds and resumed the seated position with feet lifted for 3 seconds. The sample frequency was set at 100 Hz.

Results were figured through the new plantar force visualization graph and comparison to the normal stance is established for each subject in two steps. Firstly, the evolution of the center of pressure location throughout the eleven footprints is observed. It defines the global dynamic of the foot. During normal stance, it usually shows a progressive headway along the medio-lateral axis, from the heel to the forefoot (Allard [2]). Other trajectories or headway paces could reveal pathology. Then, the shade of the eleven sensors is observed in each of the eleven footprints. During normal stance, a taligrade phase first appears for 20% of the stance phase time, then a mid-stance phase until 65% and finally a digital phase completing the 100% (Viel [8]). This normal dynamic of the foot compresses first the single heel sensors. Metatarsal heads join then for the mid stance phase. And finally, hallux and toes step on the floor before rearfoot lifts for the propulsive phase. Mid-foot areas are potentially participating in the mid-stance phase, depending on the dynamic shape of the foot: flat, normal or hollow foot as well as inversion. Any abnormal solicitation of sensor may alerts the clinician about current and/or consecutive pathologies.

4 Results

4.1 Dynamic calibration

The force/signal curves were obtained for each sensors of each slipper between 50 and 3000 N (Fig. 4). An elastic behavior was observed for every sensor as the compression phases and the release phases are perfectly superimposed. However each sensor has its own mechanical response which is not linear.

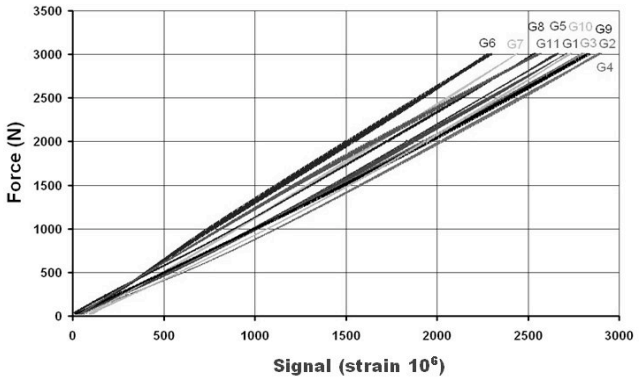

Fig. 4. Force/signal curves of the sensors of the left slipper

To best fit the sensor behavior, we approach each force/signal curve by a multi-degree equation, looking for the optimal degree to obtain minimal error. Six-degree equation appeared necessary to obtain less than 5 N of error throughout the 50-3000 N bandwidth.

The uncompressed sensors didn't show any signal variation during the calibration process whatever was the compressed sensor. That ensures the independence of each sensor and certifies that any signal variation means a direct solicitation of the sensor.

4.2 Dead load weighting

During the loading phase, the global mass measured by the sole was very similar across the 3 cycles (Fig. 5). However, measured masses were quite inaccurate: 5(±0.2) kg, 22(±0.5) kg, 31.1(±1) kg and 21.9(±0.7) kg and 5.2(±0.2) kg, instead of respectively 6, 24, 34, 24 and 6 kg. Those gaps were expected since the force/signal relationships can produce a maximal error of 5 N per sensor, according to the calibration, i.e. 55 N or 5.6 kg per slipper.

We conclude that static measurement can't be used for weighting the light loads but allow comparing two loads or the evolution of a same load.

4.3 Testing

The plantar forces visualization graph is obtained for each of the four subjects (Fig. 6).

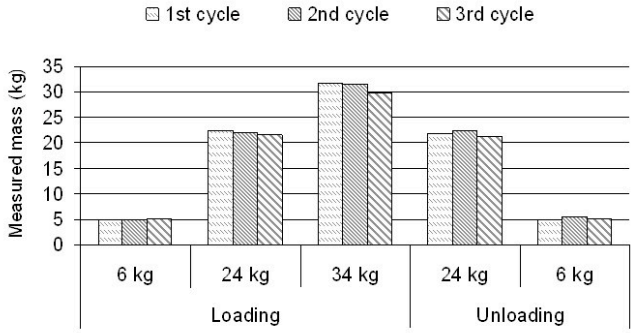

Fig. 5. Measured mass given by the slipper when loading and unloading at 6 kg, 24 kg, 34 kg, 24 kg and 6 kg, in three consecutive cycles, separated by total unloading and offset setup

The results of subject A show a difference between the feet. The left foot presents a rather normal dynamics. The center of pressure is located in the medio-lateral middle axis of the foot throughout the step and comes from the heel to the forefoot region progressively. The rearfoot contact phase takes up the first 20% of the duration of the stance phase. The full foot contact phase is spread over 50% of the stance phase, while the propulsion phase takes up the remaining 30%. However, during propulsion the third metatarsal head is more solicited (30% to 50% of the experimental mass) than the first and fifth metatarsal heads (10% to 20% of the experimental mass). This may indicate a sagging metatarsal head arch. The third metatarsal head could result in pain later in the future. The right foot shows a much abnormal dynamics. The center of pressure appears directly before the heel, which means that an isolated rearfoot contact phase does not exist. Moreover, none of the external sensors are solicited over 10% of the experimental mass. This may indicate pronation of the foot during the entire stance phase. This could be a consequence of the historic fracture and sprains of the right ankle.

The results of subject B reveal a rather normal dynamics for the right foot whereas the left foot presents a particularly long use of the rearfoot region. The medial heel still loads with 10% of the experimental mass at 80% of the stance phase duration. The very slow progression of the center of pressure confirms this phenomenon. This could be linked to the knee and ankle sprain subject B sustained in the left limb.

The results of subject C demonstrate a perfectly normal dynamics for left foot, starting at the medial heel before soliciting the lateral heel and ending with most of the force over the hallux. However, the first metatarsal head gets very little load and the hallux is bearing more than 10% of the mass as soon as 40% of the duration of the stance phase. This could lead to future hallux pain. For the right foot, the center of pressure describes a normal trajectory while, during the mid-stance phase, the forefoot is not solicited over 10% of the experimental mass and the rear part of the mid-foot is unusually constrained. This indicates a potential flatfoot behavior during the mid-stance phase. The global force can be spread over of a majority of sensors, with less than 10% of mass on most of them.

The results of subject D highlight healthy use of the left foot and possible flat foot behavior for the right foot like subject C. The right center of pressure indicates a normal roll but no sensor appeared to be more loaded than any other during the first 60% of the stance phase, except for the heel.

In all case, those results appeared thanks to the new graph and should be interpreted by competent clinicians.

5 Conclusion

Improved through a higher number of sensors and a new assembly system, instrumented slippers have ambitious baropodometric aims. Whereas the baropodometric insoles record the foot-to-sole pressure inside the shoe, the instrumented slippers acquire the foot-to-ground forces which are approaching the barefoot walking forces as the mechanical characteristics of the sole do not alter the foot contact.

As the eleven sensors cover 90% of the sole, any pathologic foot dynamics can be observed. Thanks innovating and user-friendly visualization graph, clinicians can check the evolution of the plantar force distribution throughout the entire stance phase. The instants of occurrence and duration of force exertion could be identified for every anatomic area. Symmetry of the feet can also be focused.

Calibration process ensures an error of measurement under 5 N for every of the 22 sensors solicited between 50 and 3000 N. For lighter loads, the inaccuracy increased but the measurement repeatability stays approved.

The clinical test underlined how informative the instrumented slippers coupled with the visualization graph could be. The dynamic behavior of the foot throughout the entire stance phase is easily recorded and observed at a glance. Clinician gets a new device to complete the gait diagnosis of their patients. While the subject walks, he can keep observing the global kinematics as the baropodometric device runs alone. Then, the entire treatment and the graph plotting process take less than fifteen minutes. Individual mass and trial acquired signal are the only required data. In conclusion, we improved and developed a new plantar force acquisition device and a visualization graph intended for everyday use in clinical lab.

Next step will be to miniaturize the gauge conditioner in order to insert it around the slipper and develop wireless record to quit the backpack holding.

Acknowledgments

Acknowledment goes to Arnaud Faivre who authorized this work. Fany Chedevergne received a research salary from the Ministry of National Education, Research and Technology of France to conduct this project.

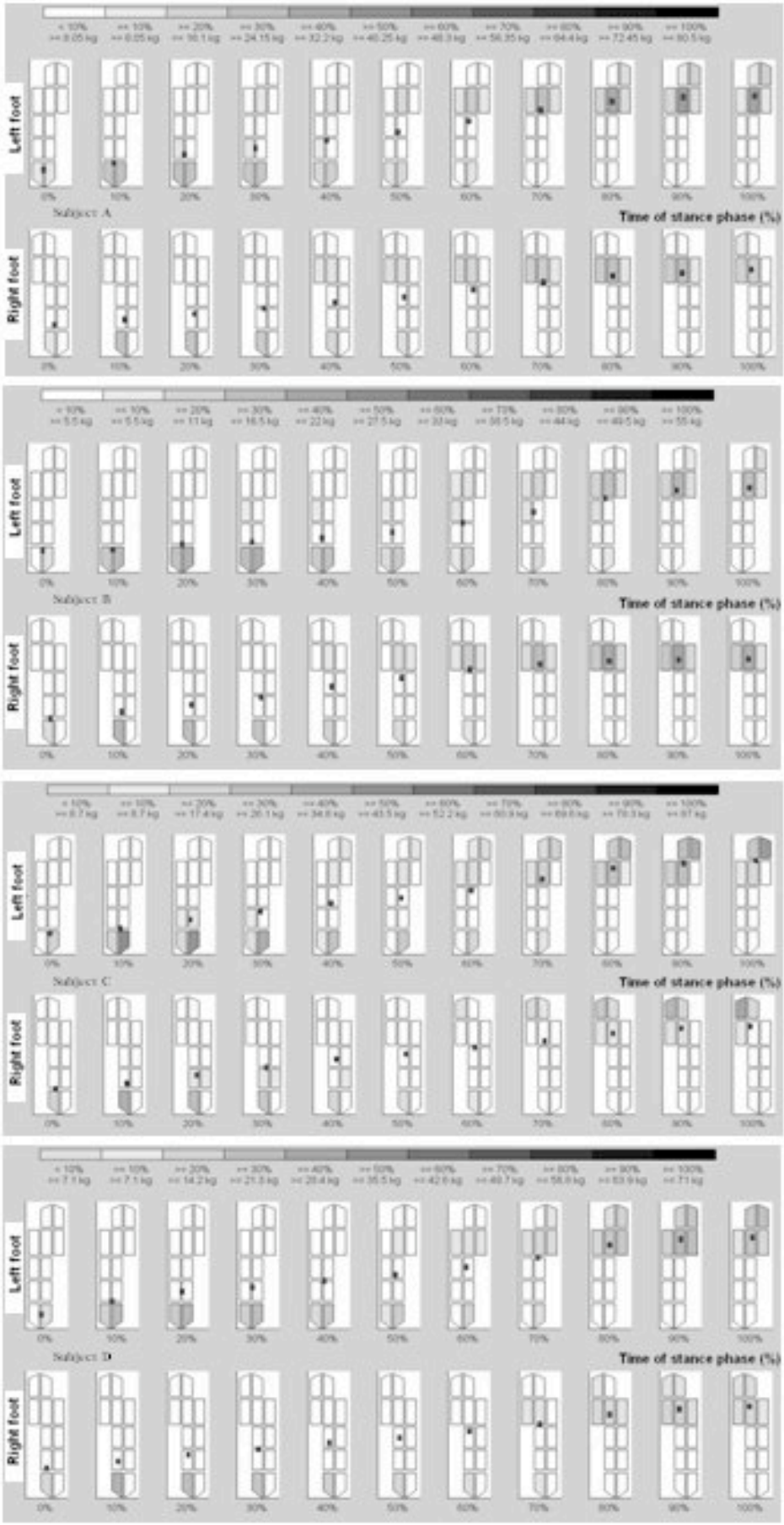

Fig. 6. Plantar force visualization graph of each subject.
Mean stance phase over the three trials of a 10-meters back walking task

References

1. C. Kowalski, *Conséquences pathologique de la brièveté des muscles gastrocnémiens*, Médecine et Chirurgie du Pied **22**(3), 159-180, (2006).
2. P. Allard, J. P. Blanchi, *La biomécanique* (Paris, France : PUF Collection Que sais-je ? 2000)
3. P.R.Cavanagh, F.G.Hewitt Jr., J.E. Perry, *In-shoe plantar pressure measurement: a review,* The Foot **2**(4), 185-194, (1992).
4. W.Herzog, B. Nigg, L.J. Read, E.Olsson, *Asymmetries in ground reaction force patterns in normal human gait*, Med. and Sci. Sport Exer. **21**, 110-114, (1989).
5. S.Meyring, R.R. Diehl, T.L.,Milani, E.M. Hennig, P. Berlit, *Dynamic plantar pressure distribution measurements in hemiparetic patient,* Clin. Biomech. **12**(1), 60-65, (1997).
6. J. Perry, *Gait Analysis. Normal and Pathological Gait* (Thorfare, USA : SLACK Incorporated, 1992)
7. J. Perttunen, *Foot loading in normal and pathological walking*. (University of Jyvaskyla, Finland : Ph.D. thesis, 2002)
8. E.Viel, *La marche humaine, la course et le saut*. (Paris, France : Masson, 2000)
9. F.A. Asphahani, H.C. Lee, *Portable system for analyzing human gait* (United States patent US6836744 B1, 2004)
10. A. Faivre, *Conception et validation d'un nouvel outil d'analyse clinique de la marche* (University of Franche-Comté , France : Ph. D. thesis, 2003)
11. T.S. Gross, R.P.Bunch, *Measurement of discrete vertical in-shoe stress with piezoelectric transducers,* J. Biomed. Eng. **10**(3), 261-265, (1988).
12. C.Kirtley, K.Tong, Insole gyro system for gait analysis, *Proceedings of the RESNA Annual Conference* (2000).
13. S.Miyazaki, H.Iwakura, *Foot-force measuring device for clinical assessment of pathological gait*, Medical and Biological Engineering and Computing **16**(4), 429-436, (1978).
14. H.S. Ranu, *Miniature load cells for the measurement of foot-ground reaction forces and centre of foot pressure during gait,* J. Biomed. Eng. **8**(2), 175-177, (1986).
15. G.A. Spolek, F.G. Lippert, *An instrumented shoe; a portable force measuring device,* Journal of Biomechanics, **9**(12), 779-783, (1976).
16. A.Faivre, M. Dahan, B.Parratte, *Instrumented shoe sole and shoe with instrumented sole*. (European patent EP1464281 B1, 2006).
17. A.Faivre, M. Dahan, B.Parratte, G. Monnier, *Instrumented shoe for pathological gait assessment,* Mechanics Research Communications **31**, 627-632, (2004).
18. C.Bertsch, H.Unger, W. Winkelmann, D. Rosenbaum, *Evaluation of early walking patterns from plantar pressure distribution measurements. First year results of 42 children,* Gait Posture **19**, 235-242, (2004).
19. E.M. Hennig, T.L. Milani, *In-shoe pressure distribution for running in various types of footwear,* J Appl Biomech, **11**(3), 299-310, (1995).
20. K.Grimmer, J. Williams, T.K. Gill, *The associations between adolescent head-on-neck posture, backpack mass, and anthropometric features,* Spine, **24**, 2262-2267, (1999).